



## Capture and release mechanism of La ions by new polyamine-based organoclays: A model system for rare-earths recovery in urban mining process

Cinzia Cristiani<sup>a,\*</sup>, Elena Maria Iannicelli-Zubiani<sup>a</sup>, Maurizio Bellotto<sup>a</sup>, Giovanni Dotelli<sup>a</sup>, Elisabetta Finocchio<sup>b</sup>, Saverio Latorrata<sup>a</sup>, Gianguido Ramis<sup>b,c</sup>, Paola Gallo Stampino<sup>a</sup>

<sup>a</sup> Politecnico Di Milano, Dipartimento Di Chimica, Materiali e Ingegneria Chimica "Giulio Natta", Piazza Leonardo Da Vinci 32, 20133, Milano, Italy

<sup>b</sup> Università Di Genova, Dipartimento Di Ingegneria Civile, Chimica e Ambientale, Via All'Opera Pia 15, 16145, Genova, Italy

<sup>c</sup> INSTM Unit, Università Di Genova, Via All'Opera Pia 15A, 16145, Genova, Italy

### ARTICLE INFO

Editor: Yunho Lee

#### Keywords:

Organoclays  
Lanthanum

Capture and release mechanism  
Recovery process urban mining

### ABSTRACT

Uptake and release capability of a new organoclay material were assessed with the final goal to evaluate its applicability in recovering REs from solutions. Capture and release capability have been tested towards a La ions model solution, and interaction mechanism and reactions, active in both capture and release processes, were related to the nature of the organoclay and the operating process parameters. The studied system, polyamine-based organoclay, is able to capture and release La ions with high efficiency. Capture involves three distinct mechanisms: ion exchange reaction with interlayer cations, surface adsorption, and finally, coordination by the polyamine. 2.5 mmol/g of amino-groups in a linear ethylene-amine based organoclay are enough to remove all the lanthanum ions in solution when contacted with containing 0.48 mmol/g<sub>clay</sub>, i.e. 2600 ppm/clay. 12 coordinating sites are needed for each lanthanum ion. Finally, the organic part of the sorbent solid is highly stable, being unmodified upon many cycles of use.

The release step is greatly pH dependent, and the optimised pH is equal to 1. Under these conditions, release efficiencies are always higher than 80 %.

Applying multiple steps and intermediate re-basification, very high and reproducible global efficiencies (up to 90 %) are reached.

## 1. Introduction

In these last centuries, technology has acquired a fast-increasing importance on everyday life: it is probably impossible for us to imagine our daily life without technological equipment. This has become much more stringent considering the 2020 pandemic. However, little attention is paid to natural resources and raw materials consumption to produce them. Humankind must win the challenges to secure a sustainable access to non-energy non-agricultural raw materials to future generations.

Circular Economy, where products, materials and resources are maintained in the use as long as possible, with minimum waste generation [1], is a tremendous opportunity to preserve the World's resources. In this respect, the approach known as "urban mining" has attracted large interest from both academia and industry. An example

can be considered the recovery and reuse of raw materials from Electric and Electronic Wastes (WEEE). WEEE are indeed generated two to three times faster than other waste streams, due both to rapid increase in consumer electronic devices, and to their ever-wider distribution [2–5]. They are dumped at landfills [6] even if they are rich in precious and strategic metals, such as Rare Earths (REs) or metals of the Pt group (PM), in many cases in higher contents than those of natural minerals [3, 7].

For these reasons, the study of efficient REs and PMs recovery from WEEE can lead to undeniable socio-economic and environmental benefits [3]. WEEE, properly treated, could be transformed into high added value economic products, minimizing environmental impacts on both production and disposal steps [8].

Some barriers to recovery and revalorization of metals in End Of Life materials are still present in all the chain of treatment, and particular

\* Corresponding author.

E-mail address: [cinzia.cristiani@polimi.it](mailto:cinzia.cristiani@polimi.it) (C. Cristiani).

<https://doi.org/10.1016/j.jece.2020.104730>

Received 7 August 2020; Received in revised form 25 October 2020; Accepted 4 November 2020

Available online 7 November 2020

2213-3437/© 2020 The Authors.

Published by Elsevier Ltd.

This is an open access article under the CC BY-NC-ND license

(<http://creativecommons.org/licenses/by-nc-nd/4.0/>).

attention has been paid to the final step, metal recovery, that can be realized by different techniques: pyrometallurgical, biometallurgical and hydrometallurgical [9–13]. Among the others, hydrometallurgical methods have been reported [2,14,15] to be one of the most interesting in view of the lower energy demand, no combustion residues and no dust emissions. However, some disadvantages are still present, i.e. large number of steps, use of chemicals, wastewater generation. Among hydrometallurgical processes, adsorption is one of the most interesting. Adsorption techniques offer unique advantages owing to the use of synthetic [11,16,17] and natural solid materials for metal removal [18–22].

Although the most widely used adsorbent is activated carbon, clay minerals have promising potential due to their high efficiency and low cost. They could be effective even with low metal ions concentration, their sorption capacity could be improved by simple modification, and their regeneration can be quite easily obtained. In particular, smectites have been proposed as absorbing materials, in view of their lamellar structure that accounts for expandable interlayer space, able to capture metal ions via ion-exchange mechanisms, but also to allow for intercalation of molecules of chelating capability [18,23]. Therefore, their natural capability to remove ions from water solutions can be enhanced this way [24–26].

In a previous paper [27] two natural standard smectites, provided by the Clay Minerals Society, namely a Ca-montmorillonite (STx-1b) and a Na rich montmorillonite (SWy-2), were used as sorbents and fully characterized. Already pristine materials showed interesting metal capture capability (20–30 %).

In the literature, clay-modified ammonium salts were reported as possible sorbents of choice for capture of metal cations in many applications [22,24,28–30].

Clay modification using polymers or surfactants of different composition, lengths and structure has been proposed by the Authors [23]. Preparation and characterization of hybrid clay-PEG (Poly-Ethylene Glycol) have been assessed and a simple and environmentally friendly procedure (water-based, room temperature) has been implemented. It has been demonstrated that PEG can be easily trapped by the clay in a stable way [31–35]. Hybrid materials based on clays and polyamines were prepared, characterized and tested [36] in the capture of La, considered as a model ion. The final material efficiency depends on a synergic effect exerted by the combined system sorbent-modifier. As modifying agents, polyamines are the better choice, in view of their capability to coordinate and capture metal ions [15,27,36–39].

In this paper, innovation regards the improvement of uptake and release capabilities of a good performant organoclay. Material is assessed, with the final goal to evaluate its applicability in REs and precious metals recovery from solutions.

From an industrial point of view, the environmental impacts associated with a designed hydrometallurgical treatment of the small WEEE has been already assessed through the Life Cycle Assessment (LCA) methodology [15]. The approach cradle-to-gate was used to design a pilot plant financed by a project of Lombardia Region (Italy) (“E-WASTE – Il ciclo intelligente” ID 40,511,448). The pilot plant was built and the process implemented in summer 2017. However, the sorbent material needs to be improved to fulfil requirements of industrial application. A deeper study is required to better control sorbent properties. Furthermore, also the comprehension of the mechanisms related to capture and release steps will boost the use of the here proposed organoclays to a wider field of application. A better knowledge of the phenomena behind the chemical process during sorption can allow for a proper design of the material to better control the process. For examples, materials with improved efficiency or lifetime could be synthesized. In addition, the reusability of the sorbent solid matrices deserves interest; indeed, if solids can be regenerated and reused, the set up for continuous processes will favor a future “circular industrial” approach.

Therefore, in this work a new organoclay has been tested to prove its capability in capture and release of metals of the REs group. Metal

adsorption mechanisms have also been studied and related to both organoclay nature and operating parameters of the process. Finally, description of metal-sorbent interaction is proposed together with suggestions on process parameters managing to optimize metal recovery.

## 2. Experimental

### 2.1. Materials

Ca-montmorillonite (STx-1b, The Clay Minerals Society, STx in the following) has been modified by intercalation with a linear commercial polyamine (99 %, supplied by Aldrich) characterized by 6 amino-groups, pentaethylenehexamine (STxL6 in the following).

From the supplier datasheet, the chemical composition of the mineral clay was:  ${}^{\text{IV}}\text{Si}_{4.0}({}^{\text{VI}}\text{Al}_{1.21}\text{Fe}^{3+}_{0.05}\text{Mg}^{2+}_{0.36}\text{Ti}_{0.02})^{\text{XII}}(\text{Ca}_{0.14}\text{Na}_{0.02}\text{K}_{0.01})\text{O}_{10}(\text{OH})_2$ .

Lanthanum (III) nitrate pentahydrate, nitric acid (99.99 %, ACS reagent) and sodium hydroxide (ACS reagent), were supplied by Sigma-Aldrich.

### 2.2. Preparation of the organoclay (STxL6)

The synthesis of the organoclay was assessed elsewhere [36]. Briefly, 2 g of clay were mixed with 50 ml of an aqueous solution of the L6 polymer, stirred with a magnetic stirrer (500 rpm), at 30 °C 90 min. Polyamine initial concentrations of 180 mmol/L and pH = 11, (measured by Mettler Toledo FE20/EL20 digital pH-meter), were applied. The solid-liquid separation was performed by centrifugation (13,000 rpm, 1 h, by a HETTICH 32 RotoFix centrifuge). Polymer content in the solid was calculated by the difference of initial and final polyamine concentrations in the liquid, determined by Chemical Oxygen Demand (COD) analysis (Spectrodirect Lovibond instrument) according to [36,40].

### 2.3. Uptake/release tests on lanthanum model solution

The uptake and release processes are sketched in Fig. 1, they were set up according to [27]; sorbent solid contained 0.4 mmol polyamine/g clay [36].

In a typical experiment, 2 g of solid were contacted with 50 ml (solid/liquid = 0.04 g/mL) of  $\text{La}(\text{NO}_3)_3$  aqueous solutions in the concentration range 10–200 mmol/L and pH = 5, i.e. pH of La initial solutions. After stirring (500 rpm) at room temperature for 90 min, the suspensions were separated by centrifugation (13,000 rpm, 1 h).

Release tests were performed according to [27] at contact time of 90 min under stirring (500 rpm), pH in the range 1–7 by  $\text{HNO}_3$  and solid/liquid ratio of 0.026 g/mL. Phases were separated by centrifugation; the liquid phase was analysed by ICP-OES inductively coupled plasma optical emission analysis (Optima 2000DV, Perkin Elmer). In both uptake and release tests, the presence of Ca and Mg was also checked.

Capture and release were assessed according to [14]:

$$\text{metal capture at time } t \ q_t = \frac{(C_0 - C_t)V}{W} \quad (1)$$

$$\text{metal release at time } t \ q_w = \frac{(C_w)V}{W} \quad (2)$$

$$\text{Uptake efficiency} = \frac{(C_0 - C_t)100}{C_0} \quad (3)$$

$$\text{Release efficiency} = \frac{(C_w)100}{C_e} \quad (4)$$

where  $q_t$  (mmol/g) and  $q_w$  were calculated from the mass balance equation,  $C_0$  and  $C_t$  are the initial and the residual metal concentrations,

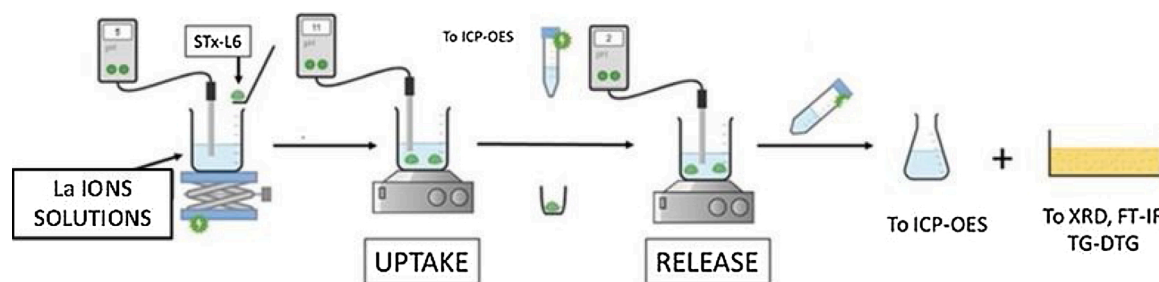


Fig. 1. Scheme of the Uptake and Release process.

$C_e$  the captured metal concentration and  $C_w$  the released metal concentration in the solutions (mmol/L) respectively,  $V$  is the volume of solution (L) and  $W$  is the mass of organoclay. Samples will be identified by labels indicating the nature of the solid and the initial molar concentration of the La solution (Table 1).

Analyses were carried out in order to verify polyamine loss during the uptake step. Amounts of polyamine, less than 10 % of the total, were found in the solutions after uptake. This data confirmed that the largest part of polyamine is not easily removable once intercalated in the clay matrix, although in the neutral form.

In the following, metal content will be expressed in terms of  $\text{mmol}/g_{\text{sorbent}}$ , which allows for direct comparison of quantitative capture between the samples.

#### 2.4. Characterizations

XRD - Powder X-ray diffraction (XRD) was performed with a Bruker D8 Advance diffractometer, (graphite monochromated, Cu-K $\alpha$  radiation, 3–30° 2 $\theta$  range, 0.02° 2 $\theta$  scan step, 1 s per step). Profiles fitted by the TOPAS P software were used for the determination of basal spacing  $d_{001}$ .

DTA-TG - Thermal analyses were performed by a DTA-TG SEIKO 6300 instrument. Experiments were performed in flowing air and temperature range of 25–1000 °C (heating rate =10 °C/min).

FT-IR analysis - Fourier transform Infrared spectra were collected in the mid-IR region using the KBr pressed disk technique (average disk weight 800 mg, 1% w/w sample powder) by a FT-IR Thermo Nicolet 380 Avatar and by a Jasco 615 spectrometer.

### 3. Results and discussion

#### 3.1. Organoclay characterization

XRD confirmed the presence of the polyamine in the clay matrix: the shift of  $d_{001}$  of the basal reflection from 15.4 Å, typical of pristine clay, to 13.7 Å, detected for the organoclay, was manifest [36]. This was confirmed by the appearance of IR absorptions in the region 3300–3200  $\text{cm}^{-1}$  (NH stretching modes), 3000–2800  $\text{cm}^{-1}$  (aliphatic CH stretching modes) and 1400–1600  $\text{cm}^{-1}$  (CH and NH deformation modes [28]). Intercalation at pH = 11, according to ICP analysis, assured that no interlayer cations displacement occurred. Therefore, being the polyamine interacting with the interlayer environment in its

Table 1  
Samples and corresponding initial La content in the uptake experiments.

Sample	Initial La concentration [mmol/L]	Initial La content [g/L]	Initial La content [mmol/ $g_{\text{STxL6}}$ ]
STxL6-10	10	1.4	0.25
STxL6-19	19	2.7	0.48
STxL6-40	40	5.5	1
STxL6-60	60	8.3	1.5
STxL6-80	80	11.1	2
STxL6-100	100	13.9	2.5
STxL6-200	200	27.8	5

neutral form, preserves the amino groups fully available for ion capture [36,39].

#### 3.2. Uptake: effect of initial lanthanum concentration and pH solutions

The uptake capability of the STxL6 organoclay towards La ions was measured by contacting the solid with nitrate solutions of increasing concentrations (10–200 mM) at pH 5, the natural value of the solutions.

Solutions pH was selected on the bases of experimental and literature considerations. Indeed, it has been reported in the literature, for similar polyamine-based organoclays, that uptake capability is pH-dependent [39]. Accordingly, La capture was performed at pH 1 and pH 11; La uptake of 0.15 and 0.30 mmol/g were measured, respectively. This effect was related to protonation degree of the polyamine which reflects on lower polyamine coordination capability at lower pH.

Therefore, reaction pH was set at 5, i.e. the pH of initial La solutions. Indeed, pH 5 was not so high to modify La species in solution, and not too low to fully protonate the polyamine. The pH evolution was monitored for all the experiments, and it naturally kept constant at about 4–5.

Specific La uptake by STxL6, as a function of different initial La content, is reported in Fig. 2.

The uptake curve of STxL6 was well fitted by an asymptotic model ( $R^2 = 0.95$ ), where the plateau value, 0.68  $\text{mmol}_{\text{La}}/g_{\text{STxL6}}$ , was reached at 2.5  $\text{mmol}_{\text{La}}/g_{\text{STxL6}}$  of initial La concentration.

A typical site saturation mechanism is manifest: at the lowest La concentrations, all the capture sites are free and able to allocate  $\text{La}^{3+}$  ions, while they are progressively saturated on increasing initial La content.

It is reported in the literature [27], that pristine clay is able to capture La ions via an exchange mechanism, where charge compensation

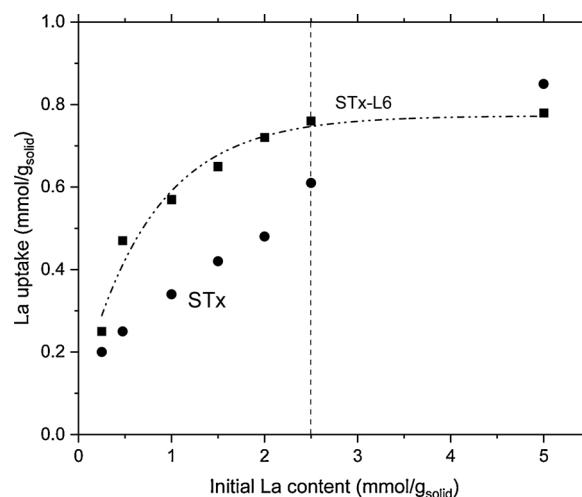


Fig. 2. La uptake- by STxL6 (square) as a function of the initial La content. (STx, circle, is reported for comparison).

allows for the interlayer electroneutrality maintenance. Ca ions are replaced by La ones, up to a threshold value of 0.54 mmol of Ca ions exchanged. Once the threshold is reached, additional La capture can occur via precipitation and/or adsorption possibly induced by ions interaction with the clay surface hydroxyls.

A similar mechanism could be hypothesized to explain STxL6 organoclay behavior. Indeed, the ion exchange capacity of the clay matrix is preserved because no charge modifications have been induced by the polyamine intercalated in the neutral form.

It is also interesting to compare the capture capability of the two solids, i.e. modified and unmodified. Within all the experimental range of concentration, before the plateau, the uptake of the unmodified STx is always quite lower than that of STxL6 (Fig. 2). Therefore, the simple ion exchange mechanism is not enough to justify the STxL6 uptake, which possibly implies the co-presence of different sites and mechanisms. Thus, the better performances of the modified materials can be associated with the presence of the polyamine. Unprotonated amino-groups, indeed, are able to interact with La ions via a mechanism that does not imply ion exchange.

To better clarify this point, physical-chemical characterization of the STxL6, before and after uptake, was performed to get information on the sites and the nature of their interaction with metal ions.

XRD analysis are reported in Fig. 3a in the region 3–10  $2^\circ\theta$ , to better evidence displacement of basal reflection maxima.

A slight, but detectable, displacement of the basal reflection position was found on increasing the captured La (Fig. 3a). Moreover, also an enlargement of the reflections was observed, suggesting the presence of some disordering phenomena [31]. Interlayer  $d_{001}$  were calculated and plotted as a function of captured La (Fig. 3b). A progressive linear decrease of the interlayer distance was found on increasing uptake from 0.25 mmol<sub>La</sub>/g<sub>STxL6</sub> up to 0.68 mmol<sub>La</sub>/g<sub>STxL6</sub>, i.e. the plateau. Once the plateau is reached, a drop of  $d_{001}$  was observed, followed by no further shrinkage of the interlayer (open squares in the figure). This behaviour suggests a change in the capture mechanism and/or the involvement of sites of different nature.

The interlayer shrinkage is an indication of new interaction. As already reported for similar systems [36], a water displacement could account for the interlayer shrinkage here observed. Indeed, La ions, when captured, can interact with both interlayer water molecules and water molecules coordinating–NH groups of the polyamine, thus displacing them. This mechanism is active only up to the site saturation, thus explaining the interlayer spacing drop and the constancy of  $d_{001}$  values afterwards. Moreover, reflection enlargement suggests disordering phenomena of the interlayers. Such a disordering phenomenon is induced by La ions randomly occupying adsorption sites.

Traces of lanthanum carbonates, (reflection at  $10.34^\circ$ , corresponding

to  $\text{La}_2(\text{CO}_3)_3 \cdot 8\text{H}_2\text{O}$ , PDF#073–0439) were sometime detected in samples after La uptake, mainly at higher La content. The presence of carbonate species, together with residual La-nitrate were also confirmed by FT-IR spectra (see below). This evidence is in line with sites saturation again:  $\text{La}^{3+}$  ions, not interacting with the interlayer due to sites total occupation, interact with the clay surface, thus becoming more accessible to atmospheric  $\text{CO}_2$ .

To verify water displacement, TG-DTG analysis was performed on STxL6 after uptake (Fig. 4 a, b).

A higher weight loss is measured for samples with higher La content, confirming the already discussed effect of initial La concentration (Fig. 4a). Moreover, a large difference in thermal decomposition behaviour was detected by DTG analysis (Fig. 4b). Such a behaviour suggests that, depending on the uptake extent, La ions are possibly interacting with different sorbent sites. Indeed, the broad decomposition temperature range observed in the curve of the solid contacted at the lower initial La concentration (30 mmol/L, black trace in the Figure) can come from the displacement of water molecules differently bonded and/or bonded at different sites. At lower La content, all the sites (exchange or coordination) are free, and the ions are able to interact with all of them.

On increasing  $\text{La}^{3+}$  uptake, a progressive occupation of the still available sites occurs; therefore, temperature range of water molecules evolution progressively is narrowed. This picture is confirmed by the DTG curve (red trace in the Figure) of the sample contacted with the intermediate initial La concentration that is the overlapping of the lowest and the highest ones (blue trace in the Figure). Once more, the co-presence of both capture mechanisms, coordination and ion exchange, is apparent.

### 3.3. Capture mechanisms

Capture of metal ions onto organoclay minerals can involve three distinct mechanisms, two of them related to clay:

- 1) ion exchange with interlayer cations [41];
- 2) surface adsorption via interaction between the clay surface hydroxyls and the metal ions [42,43];
- 3) coordination of metal ions by the amino-groups of the polyamine.

Considering that, only negligible amounts of surface La are present, mainly at the highest contact solution concentration (see crystalline La-carbonate in XRD), surface La will not be accounted for in the following.

To quantify ion exchange,  $\text{Ca}^{2+}$  and  $\text{Mg}^{2+}$  ions present in pristine organoclay and in solution after uptake were determined (Table 2). Only  $\text{Ca}^{2+}$  ions were considered to be involved in the exchange process in

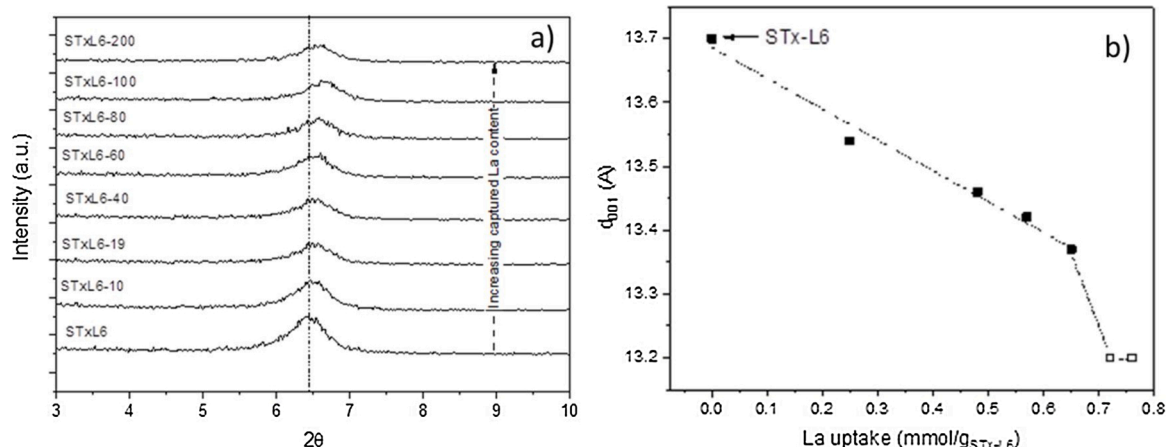


Fig. 3. a) XRD spectra of STxL6 after uptake reaction at different initial La content; b)  $d_{001}$  calculated from XRD spectra.

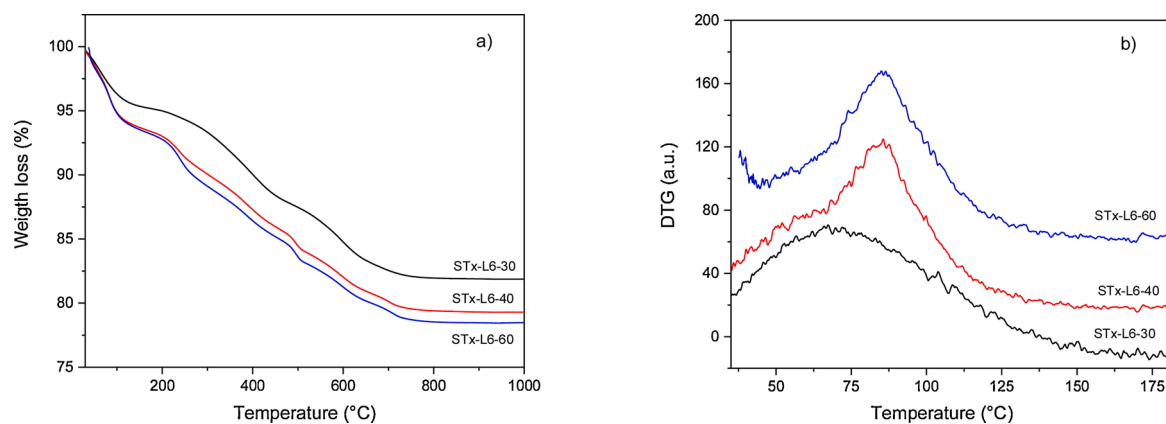


Fig. 4. TG (a) and DTG (b) of STxL6 contacted with solutions at increasing initial La concentrations.

Table 2

Composition and total charges of STxL6 after uptake reaction.

Sample	Initial La content (mmol/g)		Ions and charge distribution after uptake			
	Ca <sup>2+</sup> (mmol/g)	La <sup>3+</sup> (mmol/g)	Ca <sup>2+</sup> (charges mmol/g)	La <sup>3+</sup> (charges mmol/g)	Σ charges after uptake (mmol/g <sub>clay</sub> )	
STxL6	–	0.54	–	1.08	1.08	
STxL6–10	0.25	0.43	0.25	0.86	1.61	
STxL6–19	0.48	0.31	0.48	0.62	2.06	
STxL6–40	1	0.32	0.57	0.64	2.35	
STxL6–60	1.5	0.30	0.65	0.64	2.59	
STxL6–80	2	0.31	0.72	0.62	2.09	
STxL6–100	2.5	0.32	0.76	0.64	2.92	
STxL6–200	5	0.31	0.78	0.62	2.96	

view of the very limited and constant amount of Mg ones (0.07–0.08 mmol/g<sub>STxL6</sub>), thus negligible.

During uptake, the out-coming Ca<sup>2+</sup> are replaced by La<sup>3+</sup> to compensate the permanent negative charge of the organoclays structure and maintain electroneutrality. However, already at the lowest La concentrations (10 mmol/L), captured La in STxL6, exceeded charge compensation (1.61 for STxL6 to be compared with 1.08 of pristine STx). Hence, an additional capture mechanism must be present to account for this effect. The fraction of La<sup>3+</sup> ions captured by exchange with Ca<sup>2+</sup> can be calculated according to Eq. 5:

$$C_{La}^{exchanged} = \frac{C_{Ca}^{out} \cdot charge Ca}{charge La} \quad (5)$$

The excess La ions, resulting by the difference of the total and the exchanged ones, are therefore involved in coordination with the amino-groups (Eq. 6).

$$C_{La}^{surface adsorbed or coordinated} = C_{La}^{tot} - C_{La}^{exchanged} \quad (6)$$

Both the NH/NH<sub>2</sub> groups of the amine and the structural OHs of the clay are available for adsorption, and this second mechanism was supposed to be negligible in view of XRD results (Fig. 5).

Constant exchanged La was found at any initial concentration; conversely, coordinated La increases, up to an asymptotic value, thus suggesting the occurrence of sites saturation again. Referring to the exchange mechanism, it appears that Ca ions can be only partially exchanged and the exchange reaction is not influenced by La concentration.

As for the surface interaction mechanisms, FT-IR technique is indeed a powerful tool to investigate interaction of amines and ammonium ions with the clay matrix, as widely reported in the literature [28–30,36]. Results on the characterization of these materials are detailed in reference [36] and briefly summarized in paragraph 3.1. Moreover, spectroscopic studies can be applied to analyse the interaction of

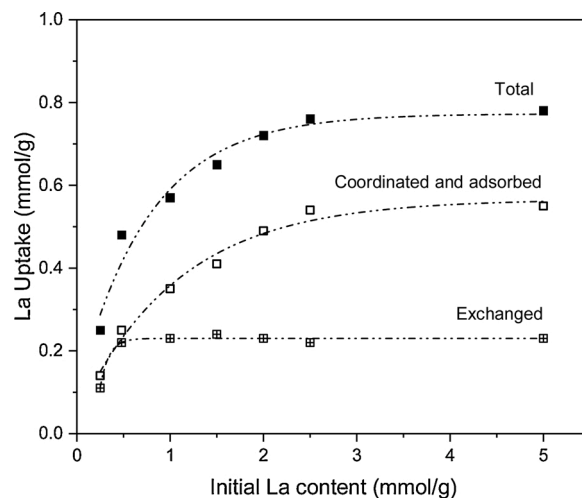


Fig. 5. Evaluation of exchanged, coordinated and adsorbed lanthanum in STxL6.

amine-based materials with metal ions in the adsorption process, with a special focus on the spectral region corresponding to surface OH groups and coordination NH sites. With this aim, FTIR spectra of STxL6 before and after La adsorption are reported in Fig. 6 and several differences, highlighted in the subtraction spectra, are pointed out.

In detail, subtraction spectrum, i.e. [spectrum of STxL6 after La ions adsorption] – [spectrum of STxL6], evidences negative bands in the region 3700–3600 cm<sup>-1</sup> and a broad absorption extending down to 3000 cm<sup>-1</sup>, pointing out that hydroxyl groups of STx matrix are involved in the interaction with La ions (surface adsorption). Moreover, negative and complex bands around 3300 cm<sup>-1</sup> (corresponding to NH stretching

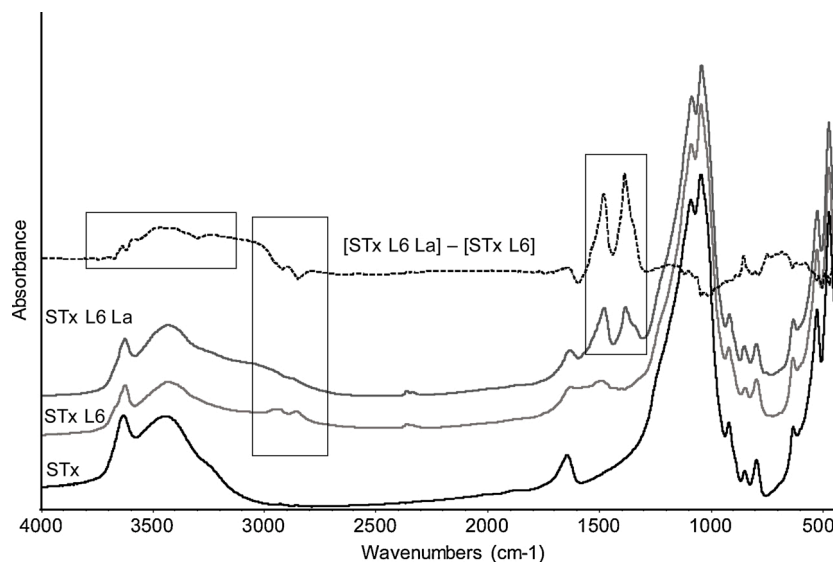


Fig. 6. FT IR skeletal spectra of STxL6 and STxL6 after  $\text{La}^{3+}$  adsorption. Dotted line: subtraction spectrum [STxL6 after La ions adsorption] – [STxL6]. The spectrum of pristine STxL6 has also been reported for comparison.

modes of amino groups in polyamine) and  $1600\text{--}1500\text{ cm}^{-1}$  (corresponding to NH deformation modes) appear, together with a broad absorption tailing towards lower frequencies. This effect is indeed due to the perturbation of amine groups signals, suggesting that also amine compounds participate to the adsorption mechanism, likely through the coordination of La ions by the nitrogen electron lone pair. In fact amine compounds are present in the clay as neutral molecules and the protonation of these molecules should occur only in very small amount during adsorption processes at  $\text{pH} = 5$  (as confirmed by the absence of significant bands associated to NH stretching vibrations characterizing ammonium ions [28]).

Also, weak negative bands can be detected in the CH stretching region. Possibly a limited fraction of alkylic chains can be involved in the mechanism or maybe are lost during the adsorption process as discussed in previous paragraph.

New strong features are detected at  $1470$  and  $1385\text{ cm}^{-1}$  with a shoulder at lower frequencies. The latter band is assigned to NO vibrational modes in nitrate species (bulk-like) which could be trapped within the clay layers (either residual La-nitrates, or Ca-nitrates). The assignment of the former band is more complex; however, considering the XRD data, and literature reports [44] this feature can be confidently assigned to vibrational modes of the  $\text{CO}_3^{2-}$  unit in carbonate species (La-carbonate and oxycarbonates) formed by  $\text{CO}_2$  chemisorption, in spite of the slightly acidic pH of the adsorption process. A component at lower frequency can also be due to some surface adsorbed carbonate species. The co-presence of both mechanisms is confirmed and discrimination of these two contributions was once more impossible.

A comparison between the uptake behaviour of pristine STx (reference) and STxL6 is reported, in Fig. 7. Ion exchange between lanthanum and interlayer cations occurs at constant extent in both the solids and accounts for about the same amount. For the STxL6 samples exchange is slightly lower, probably due to the presence of the polyamine in the interlayer which results in a steric hindrance effect.

On increasing La concentrations, different uptake trends are evident in STx and STxL6. La uptake in the pristine clay occurs linearly, while in STxL6 the already discussed asymptotic behaviour is manifest. Moreover, La uptake in STxL6 is always considerably larger. Therefore, it is reasonable to propose a key role of the coordination of metal ions by the free amino-groups.

Assuming that amine-coordinated La ions are those in excess to the exchanged ones ( $0.2\text{ mmol/g}$ ), it is possible to calculate the La coordination number. Coordinating sites available on the polyamine are equal

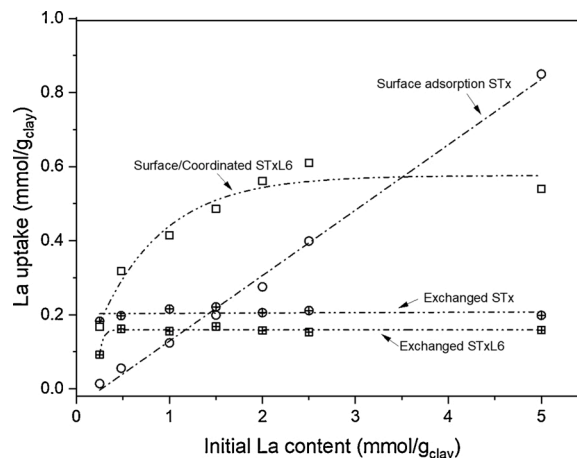


Fig. 7. Mechanisms comparison between pristine STx and modified STxL6.

to  $2.4\text{ mmol/g}$  (i.e.  $0.4\text{ mmol/g}$  of polyamine and 6 amino-groups each polyamine molecule). Supposing that all the amino-groups are involved, the coordination number of  $\text{La}^{3+}$ , at saturation, would be 12, meaning that 12 polyamine sites are coordinating each lanthanum ion, in line with literature report [45–48]. Accordingly, regarding the organoclay, the hypothesis of exchange and pure coordination, i.e. no or very limited surface adsorption, appears to be reasonable and consistent with the experimental data.

This hypothesis is also able to explain the behaviour of the materials at the highest initial concentrations (last points of Fig. 7). In that case, the pristine STx overcomes the performance of STxL6 suggesting again that surface adsorption is prevented in the latter sample.

An attempt to explain such a behaviour must consider the reaction environment of the organoclay during uptake.

Indeed, in case of STxL6, when the amino groups are highly or fully saturated by La ions, a “crowded” situation is present in the interlayer, where many positive charges surround the material. To balance the excess of positive charges, some negative ions (i.e.  $\text{NO}_3^-$ ) are attracted from the bulk of the solution to the surface. This “double layer” formed in STxL6, could possibly prevent further La ions diffusion towards the clay surface, thus hindering surface adsorption. This effect is absent, or it is very limited, in the case of pristine STx where no ions coordination can

occur.

### 3.4. Release mechanism

As discussed above, the capture of  $\text{La}^{3+}$  is supposed to involve both ion exchange and coordination mechanisms. Both interactions can be affected by pH: Ca ions can be exchanged by protons [14,39], while amino-groups can be protonated/deprotonated.

Release tests were performed by contacting 1.3 g of the lanthanum enriched STxL6 organoclays with 50 ml solutions at different initial pH, namely 1, 5, and 7, at room temperature and 90 min of contact time.

High efficiency, up to 80 %, in Lanthanum release was obtained only at very acid conditions, achieving efficiency at pH 1. In these conditions, lanthanum release occurs via protonation of the amino groups, and lanthanum exchange with protons in the interlayer. Similar release behaviour was observed in pristine clays, where the highest release efficiency (60–70 %) was found at pH 1 as well [14,39]. Accordingly, in the practice, release was always performed at pH 1.

In Fig. 8 release as a function of the uptake is plotted for STxL6 and compared with STx.

A linear trend can be evidenced in both STx and STxL6: the more the lanthanum capture, the more the released one, confirming that the desorption mechanisms is pH-dependent.

Considering the slopes of the fitted lines, a more efficient release mechanism is active in the case of the modified clay. This behaviour is supposed to be due to coordinated La and its release via protonation of the amino-groups, very fast and efficient.

After the release procedure, FT-IR spectra (not reported) evidenced that the strong band due to nitrate groups is still detectable, and its intensity is even enhanced, due to the treatment in the  $\text{HNO}_3$  aqueous solution, whereas, the band related to carbonate species disappears due to the decomposition of such species at low pH. This confirms that all the La ions could actually be recovered in this step. Correspondingly, bands due to amino-groups are not recovered, neither in the high frequency region nor in the low frequency one of the spectra. Indeed, the low pH of the release solution leads to the protonation of the amino-groups, protons replacing La ions are responsible for La recovery.

## 4. Towards industrial application

### 4.1. Solids reusability

The first assessed issue was sorbent solid reusability, i.e. the possibility to regenerate the solid matrices and to apply it in a number of subsequent cycles. Indeed, in an industrial perspective, solids that can be regenerated and reused are making the difference, both for matter of

cost, and for scale up and the setting up of continuous processes.

Therefore, solid reusability was evaluated by performing subsequent uptake and release steps on the same solid, i.e. the sorbent after a release step was used for the next uptake and release step, for a fixed number of cycles. The different cycles were evaluated in terms of global efficiency (Eq. 7), considering both the uptake and the release steps:

$$\text{Global efficiency} = \text{Uptake efficiency} \cdot \text{release efficiency} \quad (7)$$

Global efficiencies of about 65 % and 3% were found for cycle I and II, respectively which corresponded to a global efficiency of 34 %. The low overall “I + II cycles” efficiency is clearly due to the almost total inefficiency of the system at the second cycle. The collapse of the global efficiency of the second cycle is remarkable, meaning that the organoclay suffers for the operating conditions. The reasons for this behaviour are to be found in the release operation carried out at  $\text{pH} = 1$ . At this pH, the protonation of the amino groups occurs as demonstrated by the release of the captured ions. However, once protonated, the amino groups are no longer able to coordinate the metal ions, giving rise to the decrease of efficiency in the second cycle.

The excellent performance obtained in the first cycle induced to propose some solutions to accomplish organoclay reusability by solving amino-groups protonation during the first release step. Thus, before starting the new recovery cycle, the organoclay underwent an intermediate re-basification step, between release of cycle I and uptake of cycle II, in order to restore the amino-groups. Sodium hydroxide solution ( $\text{pH} = 9$ ), at room temperature, contact time of 90 min and vigorous stirring (about 700 rpm) were used for this purpose.

The increase in the overall efficiency of the “I + II cycles” was evident: an overall efficiency of the “I + II cycles” with intermediate basification was over 75 %, to be compared with 34 % without basification. The marked improvement demonstrates that the intermediate basification ensures the reactivation of the coordination functions of the polyamine (i.e.  $\text{NH}/\text{NH}_2$ ) groups. The effect of intermediate basification was tested and proved in a number of cycles equal to 4. The four-cycles process was performed according to the procedure previously reported for the two-cycles one, by keeping constant the solid/liquid ratio. Very high and reproducible global efficiencies (in the range of 80–90 %) were measured, thus confirming the stability of the solid under the operating conditions upon repeated cycles (Fig. 9).

These results confirmed once again the capability of the solid towards La ions recovery, once fixed an intermediate basification step to regenerate polyamine capture function.

Applying this process, it was experimentally demonstrated that starting with a contacting solution containing 270 mg/g of La, 237 mg can be recovered by using the same solid and applying 4 cycles with

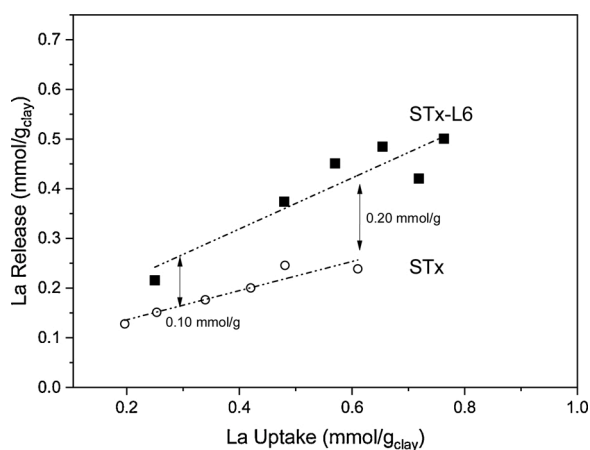


Fig. 8. La release as a function of La uptake for STxL6 (STx is reported for comparison).

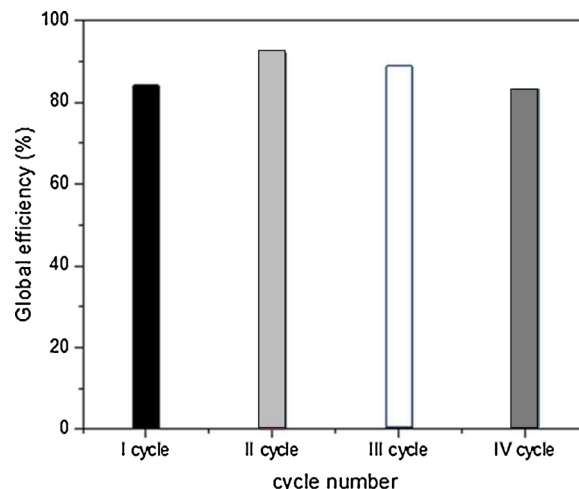


Fig. 9. Global efficiencies (uptake + release) of STxL6 for four recovery cycles.

intermediate re-basification.

These results, although preliminary, point out the possibility to apply the material in a continuous process, as it is commonly preferred at industrial level.

## 5. Conclusions

- The polyamine-based organoclay here proposed is able to capture and release La ions with high efficiency.
- Capture involves three distinct mechanisms, where two of them are related to the clay matrix. One is La exchange reaction with inter-layer Ca ions, another is surface adsorption, by means of complexes formed between the clay surface hydroxyl groups, the third one is related to the polyamine coordination properties towards metal ions.
- On increasing La concentrations, different uptake trends are evident in STx and STxL6. La uptake in the pristine clay occurs linearly, while in STxL6 an asymptotic behaviour is manifest.
- La uptake in STxL6 is always considerably larger. Therefore, it is reasonable to propose a key role of the coordination of metal ions by the free amino-groups.
- Concerning the organoclay, the hypothesis of exchange and pure coordination, i.e. no or very limited surface adsorption, appears to be reasonable and consistent with the experimental data.
- 2.5 mmol/g of amino-groups in a linear ethylene-amine based organoclay are enough to remove (with surface adsorption and ion exchange anyway occurring) all the lanthanum ions in a 19 mmol/L solution (corresponding to 0.48 mmol/g<sub>clay</sub> and to 2600 ppm/clay).
- From first estimations, 12 coordinating sites are needed for each lanthanum ion. Finally, the organic part of the sorbent solid is highly stable, being unmodified upon many cycles of use.
- The optimised parameter for the release step is pH = 1: at this pH the release efficiencies are always higher than 80 % confirming that the release phase is greatly pH dependent.
- Re-basification is required to restore the polyamine coordination function, which results fully protonated after the release process at pH 1.
- Very high and reproducible global efficiencies (about 80–90 %) are reached upon repeated cycles when an intermediate re-basification step is performed to regenerate the polyamine capture functions.
- The reusability of the sorbent solid matrices points out a possible application in continuous processes, which would favor a future “circular industrial” approach.

## CRedit authorship contribution statement

**Cinzia Cristiani:** Conceptualization, Methodology, Supervision, Writing - review & editing. **Elena Maria Iannicelli-Zubiani:** Investigation, Methodology, Validation, Writing - original draft. **Maurizio Bellotto:** Validation, Formal analysis. **Giovanni Dotelli:** Validation, Formal analysis, Funding acquisition. **Elisabetta Finocchio:** Investigation, Validation, Supervision, Writing - review & editing. **Saverio Latorrata:** Data curation, Investigation. **Gianguido Ramis:** Validation, Writing - review & editing. **Paola Gallo Stampino:** Resource, Data curation.

## Declaration of Competing Interest

The authors declare that they have no known competing financial interests or personal relationships that could have appeared to influence the work reported in this paper.

## Acknowledgments

This activity has received funding from the European Institute of Innovation and Technology (EIT). This body of the European Union receives support from the European Union’s Horizon 2020 research and

innovation programme.

Miss Giuseppina Gasti and Miss Gigliola Clerici are kindly acknowledged for their help in Thermal analysis and X-ray diffraction measurements.

## References

- [1] Circular Economy Action Plan, <http://www.consilium.europa.eu>, (n.d.).
- [2] M. Kaya, Recovery of metals and nonmetals from electronic waste by physical and chemical recycling processes, *Waste Manag.* 57 (2016) 64–90, <https://doi.org/10.1016/j.wasman.2016.08.004>.
- [3] F. Cucchiella, I. D’Adamo, S.C. Lenny Koh, P. Rosa, Recycling of WEEEs: an economic assessment of present and future e-waste streams, *Renewable Sustainable Energy Rev.* (2015), <https://doi.org/10.1016/j.rser.2015.06.010>.
- [4] S.C. Gutiérrez-Gutiérrez, F. Coulon, Y. Jiang, S. Wagland, Rare earth elements and critical metal content of extracted landfilled material and potential recovery opportunities, *Waste Manag.* (2015), <https://doi.org/10.1016/j.wasman.2015.04.024>.
- [5] B. Tansel, From electronic consumer products to e-wastes: global outlook, waste quantities, recycling challenges, *Environ. Int.* (2017), <https://doi.org/10.1016/j.envint.2016.10.002>.
- [6] S. Ilyas, J.C. Lee, B.S. Kim, Bioremoval of heavy metals from recycling industry electronic waste by a consortium of moderate thermophiles: process development and optimization, *J. Clean. Prod.* (2014), <https://doi.org/10.1016/j.jclepro.2014.02.019>.
- [7] M. Bigum, L. Brogaard, T.H. Christensen, Metal recovery from high-grade WEEE: a life cycle assessment, *J. Hazard. Mater.* (2012), <https://doi.org/10.1016/j.jhazmat.2011.10.001>.
- [8] V. Innocenzi, I. De Michelis, B. Kopacek, F. Vegliò, Yttrium recovery from primary and secondary sources: a review of main hydrometallurgical processes, *Waste Manag.* (2014), <https://doi.org/10.1016/j.wasman.2014.02.010>.
- [9] A.K. Awasthi, J. Li, An overview of the potential of eco-friendly hybrid strategy for metal recycling from WEEE, *Resour. Conserv. Recycl.* (2017), <https://doi.org/10.1016/j.resconrec.2017.07.014>.
- [10] D. Ibanescu, D. Cailan (Gavrilescu), C. Teodosiu, S. Fiore, Assessment of the waste electrical and electronic equipment management systems profile and sustainability in developed and developing European Union countries, *Waste Manag.* (2018), <https://doi.org/10.1016/j.wasman.2017.12.022>.
- [11] M.A.O. Lourenço, P. Figueira, E. Pereira, J.R.B. Gomes, C.B. Lopes, P. Ferreira, Simple, mono and bifunctional periodic mesoporous organosilicas for removal of priority hazardous substances from water: the case of mercury(II), *Chem. Eng. J.* (2017), <https://doi.org/10.1016/j.cej.2017.04.005>.
- [12] A. Priya, S. Hait, Comparative assessment of metallurgical recovery of metals from electronic waste with special emphasis on bioleaching, *Environ. Sci. Pollut. Res.* (2017), <https://doi.org/10.1007/s11356-016-8313-6>.
- [13] G.I. Zlamparet, W. Ijomah, Y. Miao, A.K. Awasthi, X. Zeng, J. Li, Remanufacturing strategies: a solution for WEEE problem, *J. Clean. Prod.* (2017), <https://doi.org/10.1016/j.jclepro.2017.02.004>.
- [14] E.M. Iannicelli-Zubiani, C. Cristiani, G. Dotelli, P. Gallo Stampino, Recovery of valuable metals from electronic scraps by clays and organo-clays: study on bi-ionic model solutions, *Waste Manag.* (2017), <https://doi.org/10.1016/j.wasman.2016.07.035>.
- [15] E.M. Iannicelli-Zubiani, M.I. Giani, F. Recanati, G. Dotelli, S. Puricelli, C. Cristiani, Environmental impacts of a hydrometallurgical process for electronic waste treatment: A life cycle assessment case study, *J. Clean. Prod.* (2017), <https://doi.org/10.1016/j.jclepro.2016.10.040>.
- [16] B. Fresco-Cala, S. Cárdenas, Potential of nanoparticle-based hybrid monoliths as sorbents in microextraction techniques, *Anal. Chim. Acta* (2018), <https://doi.org/10.1016/j.aca.2018.05.069>.
- [17] A. Jawad, L. Peng, Z. Liao, Z. Zhou, A. Shahzad, J. Iftikhar, M. Zhao, Z. Chen, Z. Chen, Selective removal of heavy metals by hydrotalcites as adsorbents in diverse wastewater: different intercalated anions with different mechanisms, *J. Clean. Prod.* (2019), <https://doi.org/10.1016/j.jclepro.2018.11.234>.
- [18] M. Claverie, J. Garcia, T. Prevost, J. Brendlé, L. Limousy, Inorganic and hybrid (organic-inorganic) lamellar materials for heavy metals and radionuclides capture in energy wastes management-A review, *Materials* (Basel). (2019), <https://doi.org/10.3390/ma12091399>.
- [19] H. Han, M.K. Rafiq, T. Zhou, R. Xu, O. Mašek, X. Li, A critical review of clay-based composites with enhanced adsorption performance for metal and organic pollutants, *J. Hazard. Mater.* (2019), <https://doi.org/10.1016/j.jhazmat.2019.02.003>.
- [20] Z. Li, P.H. Chang, W.T. Jiang, Mechanisms of Cu<sup>2+</sup>, triethylenetetramine (TETA), and Cu-TETA sorption on rectorite and its use for metal removal via metal-TETA complexation, *J. Hazard. Mater.* (2019), <https://doi.org/10.1016/j.jhazmat.2019.03.085>.
- [21] O.A. Oyewo, M.S. Onyango, C. Walkersdorfer, Adsorptive performance of surface-modified montmorillonite in vanadium removal from mine water, *Mine Water Environ.* (2017), <https://doi.org/10.1007/s10230-017-0475-z>.
- [22] X. Liu, F. Zhou, R. Chi, J. Feng, Y. Ding, Q. Liu, Preparation of modified montmorillonite and its application to rare earth adsorption, *Minerals* (2019), <https://doi.org/10.3390/min9120747>.
- [23] E.M. Iannicelli Zubiani, C. Cristiani, G. Dotelli, P.G. Stampino, R. Pelosato, Recovery of rare earths and precious metals from waste electrical and electronic

- equipment by acid leaching and immobilized chelating agents, *Chem. Eng. Trans.* (2015), <https://doi.org/10.3303/CET1543403>.
- [24] Q. Wang, S.M. Shaheen, Y. Jiang, R. Li, M. Slaný, H. Abdelrahman, E. Kwon, N. Bolan, J. Rinklebe, Z. Zhang, Fe/Mn- and P-modified drinking water treatment residuals reduced Cu and Pb phytoavailability and uptake in a mining soil, *J. Hazard. Mater.* (2021), <https://doi.org/10.1016/j.jhazmat.2020.123628>.
- [25] W. Du, X. Wang, G. Chen, J. Zhang, M. Slaný, Synthesis, property and mechanism analysis of a novel polyhydroxy organic amine shale hydration inhibitor, *Minerals* (2020), <https://doi.org/10.3390/min10020128>.
- [26] W. Du, M. Slaný, X. Wang, G. Chen, J. Zhang, The inhibition property and mechanism of a novel low molecularweight zwitterionic copolymer for improving wellbore stability, *Polymers* (Basel). (2020), <https://doi.org/10.3390/polym12030708>.
- [27] E.M. Iannicelli-Zubiani, C. Cristiani, G. Dotelli, P. Gallo Stampino, R. Pelosato, E. Mesto, E. Schingaro, M. Lacialamita, Use of natural clays as sorbent materials for rare earth ions: materials characterization and set up of the operative parameters, *Waste Manag.* (2015), <https://doi.org/10.1016/j.wasman.2015.09.017>.
- [28] M. Slaný, Ľ. Jankovič, J. Madejová, Structural characterization of organo-montmorillonites prepared from a series of primary alkylamines salts: Mid-IR and near-IR study, *Appl. Clay Sci.* (2019), <https://doi.org/10.1016/j.clay.2019.04.016>.
- [29] J. Madejová, udmila Sekeráková, V. Bizovská, M. Slaný, uboš Jankovič, Near-infrared spectroscopy as an effective tool for monitoring the conformation of alkylammonium surfactants in montmorillonite interlayers, *Vib. Spectrosc.* (2016), <https://doi.org/10.1016/j.vibspec.2016.02.010>.
- [30] J. Madejová, M. Jankovič, V. Slaný, Hronský, Conformation heterogeneity of alkylammonium surfactants self-assembled on montmorillonite: effect of head-group structure and temperature, *Appl. Surf. Sci.* (2020), <https://doi.org/10.1016/j.apsusc.2019.144125>.
- [31] E. Finocchio, I. Baccini, C. Cristiani, G. Dotelli, P. Gallo Stampino, L. Zampori, Hybrid organo-inorganic clay with nonionic interlayers. Mid- and near-IR spectroscopic studies, *J. Phys. Chem. A* (2011), <https://doi.org/10.1021/jp200845e>.
- [32] E. Finocchio, C. Cristiani, G. Dotelli, P.G. Stampino, L. Zampori, Thermal evolution of PEG-based and BRIJ-based hybrid organo-inorganic materials. FT-IR, *Vib. Spectrosc.* (2014), <https://doi.org/10.1016/j.vibspec.2013.12.010>.
- [33] L. Zampori, G. Dotelli, P. Gallo Stampino, C. Cristiani, F. Zorzi, E. Finocchio, Thermal characterization of a montmorillonite, modified with polyethylene-glycols (PEG1500 and PEG4000), by in situ HT-XRD and FT IR: formation of a high-temperature phase, *Appl. Clay Sci.* (2012), <https://doi.org/10.1016/j.clay.2012.02.015>.
- [34] L. Zampori, P.G. Stampino, C. Cristiani, P. Cazzola, G. Dotelli, Intercalation of poly (ethylene-oxides) in montmorillonite: tailor-made nanocontainers for drug delivery systems, *Appl. Clay Sci.* (2010), <https://doi.org/10.1016/j.clay.2010.08.009>.
- [35] L. Zampori, P.G. Stampino, C. Cristiani, G. Dotelli, P. Cazzola, Synthesis of organoclays using non-ionic surfactants: effect of time, temperature and concentration, *Appl. Clay Sci.* (2010), <https://doi.org/10.1016/j.clay.2009.11.015>.
- [36] C. Cristiani, E.M. Iannicelli-Zubiani, G. Dotelli, E. Finocchio, P.G. Stampino, M. Licchelli, Polyamine-based organo-clays for polluted water treatment: effect of polyamine structure and content, *Polymers* (Basel). (2019), <https://doi.org/10.3390/polym11050897>.
- [37] E.M. Iannicelli-Zubiani, P. Gallo Stampino, C. Cristiani, G. Dotelli, Enhanced lanthanum adsorption by amine modified activated carbon, *Chem. Eng. J.* (2018), <https://doi.org/10.1016/j.cej.2018.01.154>.
- [38] E.M. Iannicelli-Zubiani, C. Cristiani, G. Dotelli, P.G. Stampino, Solid sorbents for rare earths recovery from electronic waste. *Wastes Solut. Treat. Oppor. - Sel. Pap. From 3rd Ed. Int. Conf. Wastes Solut. Treat. Oppor.*, 2015, <https://doi.org/10.1201/b18853-60>, 2015.
- [39] E.M. Iannicelli-Zubiani, C. Cristiani, G. Dotelli, P.G. Stampino, R. Pelosato, E. Finocchio, Effect of pH in the synthesis of organo-clays for rare earths removal, *Environ. Eng. Manag. J* (2017), <https://doi.org/10.30638/eemj.2017.187>.
- [40] ASTM, *Standard Test Methods for Chemical Oxygen Demand (Dichromate Oxygen Demand) of Water*, 2006.
- [41] A. Djukić, U. Jovanović, T. Tuvić, V. Andrić, J. Grbović Novaković, N. Ivanović, L. Matović, The potential of ball-milled Serbian natural clay for removal of heavy metal contaminants from wastewaters: simultaneous sorption of Ni, Cr, Cd and Pb ions, *Ceram. Int.* (2013), <https://doi.org/10.1016/j.ceramint.2013.02.061>.
- [42] K. Dimos, P. Stathi, M.A. Karakassides, Y. Deligiannakis, Synthesis and characterization of hybrid MCM-41 materials for heavy metal adsorption, *Microporous Mesoporous Mater.* (2009), <https://doi.org/10.1016/j.micromeso.2009.05.021>.
- [43] J. Ikhsan, J.D. Wells, B.B. Johnson, M.J. Angove, Surface complexation modeling of the sorption of Zn(II) by montmorillonite, *Colloids Surf. A Physicochem. Eng. Asp.* (2005), <https://doi.org/10.1016/j.colsurfa.2004.10.011>.
- [44] T. Le Van, M. Che, J.M. Tatibouët, M. Kermarec, Infrared study of the formation and stability of La<sub>2</sub>O<sub>2</sub>CO<sub>3</sub> during the oxidative coupling of methane on La<sub>2</sub>O<sub>3</sub>, *J. Catal.* (1993), <https://doi.org/10.1006/jcat.1993.1185>.
- [45] E. Bodo, Lanthanum(III) and lutetium(III) in nitrate-based ionic liquids: a theoretical study of their coordination shell, *J. Phys. Chem. B* (2015), <https://doi.org/10.1021/acs.jpcc.5b06387>.
- [46] C.H. Kim, S.G. Lee, *Crystal structure and thermal properties of the lanthanum(III) complex with triethylenetetraaminehexaacetic acid: K<sub>3</sub>[La(TTHA)]·5H<sub>2</sub>O*, *Bull. Korean Chem. Soc.* (1999).
- [47] B. Li, H.M. Wen, Y. Cui, G. Qian, B. Chen, Multifunctional lanthanide coordination polymers, *Prog. Polym. Sci.* (2015), <https://doi.org/10.1016/j.progpolymsci.2015.04.008>.
- [48] W. Zheng, L. Liu, X. Zhao, J. He, A. Wang, T.W. Chan, S. Wu, Effects of lanthanum complex on the thermo-oxidative aging of natural rubber, *Polym. Degrad. Stab.* (2015), <https://doi.org/10.1016/j.polymdegradstab.2015.07.024>.